Clays Clay Miner., Vol. 71, No. 2:143–165, 2023
https://doi.org/10.1007/s42860-023-00240-w

ORIGINAL PAPER

# Ceramics Properties of Indurated-Shale Quarry Wastes from Abakaliki, Southeastern Nigeria: Application as Raw Materials in Roofing-Tile Production

**Obisi M. Nweke · Adolphus I. Omeokachie**

Accepted: 29 May 2023 / Published online: 6 July 2023


**Abstract** The present study describes research carried out to evaluate the mineralogical, geochemical and technological properties of indurated shale-quarry wastes and assess the suitability of these low-cost and locally available quarry wastes generated from crushed indurated shales for possible use as alternatives to fresh raw materials in the manufacture of roofing-tile products. Firstly, the mineralogical and chemical properties of the indurated shales were investigated by X-ray diffraction (XRD) and X-ray fluorescence, while their physical properties were identified by grain-size distribution, Atterberg limits, and clay activity. Samples of indurated shale-quarry wastes (ISQWs) were subjected to heat treatment at elevated firing temperatures to provide the required strength and durability and their ceramics properties (linear shrinkage, weight loss, water absorption, bulk density, and flexural strength) were determined. From the results, the ISQWs were composed predominantly of fine particles with medium plasticity and clay activity with values generally > 0.75. The mineralogy revealed a predominance of aluminosilicates (illite-kaolinite-smectite-chlorite) with large quartz contents and variable percentages of carbonate and feldspar. The oxides were dominated by $SiO_2$ and $Al_2O_3$, small amounts of ferromagnesian minerals, and considerable amounts of alkalis ($K_2O$ and $Na_2O$) which act as fluxes. The CaO concentrations were variable and related to carbonate contents. Characterizations based on compositional ternary (total clay mineral-carbonate-quartz + feldspar) systems, Casagrande clay workability charts, and Winkler and McNally diagrams revealed their suitability for ceramics applications as the majority of ISQW samples fell within the specifications for roofing tiles. The ISQWs fired at a high temperature of 1000°C revealed considerable weight loss, reduction in both linear shrinkage and water absorption with insignificant increase in flexural strength. In order to achieve excellent ceramics properties and further reduce sintering temperature for their suitability as raw materials in the production of roofing tiles, beneficiations of ISQWs are highly recommended.

**Keywords** Albian · Asu River Group · Heat treatment · Indurated shale · Roofing tiles · Sustainable · Temperature

**Supplementary Information** The online version contains supplementary material available at https://doi.org/10.1007/s42860-023-00240-w.

O. M. Nweke (✉)
Department of Geology and Exploration Geophysics, Ebonyi State University, Abakaliki, Nigeria
e-mail: nwaekeoby@yahoo.com

A. I. Omeokachie
Department of Geological Sciences, Nnamdi Azikwe University, Awka, Nigeria

## Introduction

Conventional roofing tiles are usually composed of either clayey or concrete materials which are strong, durable, and non-combustible. According to Diko-Makia and Ligege (2020), Terrones-Saeta et al. (2020) and Revuelta (2021), ceramic roofing tiles are typical building materials, manufactured from raw materials such as clays, shale, silica, fluxes (feldspars), or similar naturally occurring earthy substances and subjected to heat treatment at elevated temperatures (firing). They have been used for centuries both in residential- and commercial-property applications and are considered to be environmentally friendly roofing materials, which contribute greatly to the creation of a favorable microclimate (local region with unique pattern of weather different from local climate) (Pavlova et al., 2019). They have significant advantages over other types of roofing tiles not only in terms of architectural expression and durability but also in terms of other physical and mechanical characteristics which have greatly influenced their widespread adoption among builders. The exploitation of clay materials for industrial end-products such as structural ceramics (bricks and floor and roofing tiles) and earthenware (porcelain, household ceramics), are based on the availability of raw materials, accessibility, and comparatively low to intermediate firing temperatures (Diko-Makia & Legege, 2020; Serra et al., 2013). The relevance of clays in economic (Ekosse, 2010; Kühnel, 1990; Murray, 2000) and technological development (Baccour et al., 2009; Kagonbe et al., 2021; Pavlova et al., 2019) is due to their plasticity, inertness, and stability, providing specific properties including rheology, for specific industrial use. Demand for clays as raw materials for commercial applications has risen sharply due to the rapid increase in construction owing to globalization and urbanization (Ekosse, 2010; Stock, 2012; Baraldi, 2018; Akintola et al., 2020; Terrones-Saeta et al., 2020). Globally, such impressive infrastructural growth raised demand for clays as raw materials to an estimate of 230 million tons per year (Stock, 2012; Baraldi, 2018). In Brazil, for instance, structural ceramics industries currently consume ~1.5 million $m^3$/year of clay as a raw material (Teixera et al., 2001). In the African continent, production of roofing tiles in 2019 was estimated at ~759 million $m^2$. Besides Egypt with an estimated production of 300 million $m^2$ and Nigeria with an estimated production of 115 million $m^2$, growth in production of ceramics roofing tiles has continued greatly in Sub-Saharan Africa (Stock, 2012; Baraldi, 2018). Research by Revuelta (2021) revealed that the life span of ceramic roofing tiles averaged 75 years, highlighting their durability, and they are easily recycled at the end of their service life. To continue to manufacture ceramic products, and given that clays as raw materials may become scarce in the future (Gonzales et al., 1990; Kazmi et al., 2016; Subashi De Silva & Malwatta, 2018; Terrones-Saeta et al., 2020) and considering that China has already imposed a limit on production due to insufficient raw materials (Chen et al., 2011; Lingling et al., 2005; Terrones-Saeta et al., 2020), an urgent need exists to source cheap, locally available, and sustainable raw materials that can meet the requirements of conventional, depleting natural resources, especially in tropical developing countries.

### Previous Studies of Wastes and Source of Indurated Shale

With the innovation of 'waste to wealth' technology, evaluating all possible alternative materials (which may be either wastes or unusable materials) which require less energy for manufacture and which offer excellent properties to ensure better fired products is imperative. Nowadays, many kinds of wastes are found in various categories at various locations and with various properties. Work by Ripoli (1997) on waste materials from crushed rocks showed that they can be used to replace conventional fluxing materials, especially when the wastes have the advantage of controlling the plasticity and shrinkage of the ceramics ware without producing any negative effects. Studies were carried out by Çolak and Özkan (2011) and by Özkan (2014) on the sintering properties of the Bornova shale (Turkey); those authors recommended them for possible use in the production of red fired ceramics when beneficiated. The tertiary volcanic cones at Limbe (Cameroon) were suggested by Diko-Makia and Ligege (2020) as raw materials in the ceramics industry. All these case studies showed favorable conditions for waste-recovery systems which would help to minimize the adverse effects of wastes on the environment. In all of those previous studies, characterization of the raw materials was considered vital to ascertaining their best use in the



https://doi.org/10.1007/s42860-023-00240-w Published online by Cambridge University Press

final industrial products. The Abakaliki region (southeastern Nigeria) has enormous rock reserves that are used as sources of construction aggregate (Fig. 1a). The Albian indurated shales are widely deposited in the sedimentary basins of southeastern Nigeria and have been studied by Obiora and Charan (2011), Nweke and Okogbue (2017), and Nweke and Okogbue (2021) and were estimated to cover ~ 452 km$^2$. Commercial, mechanized crushing of the Albian indurated shales and other rock types such as pyroclastics, limestones, and sandstones are carried out at Ebonyi State Umuoghara industrial clusters, on the outskirts of the Abakaliki Township. According to Nweke and Okogbue (2017) the volumes of indurated shale that are quarried, processed, and utilized annually as construction aggregates are increasing rapidly and ~ 15,000 metric tons of crushed aggregates are usually produced on a daily basis. During the quarrying and crushing, huge quantities of wastes (i.e. by-products of the crushed indurated shale referred to locally as 'dust') are usually generated on a daily basis and are considered toxic and environmentally harmful (Okogbue & Nweke, 2018). These harmful quarry wastes (Fig. 1b, c) are occasionally discarded into abandoned lands and often in tailings dams, thereby posing serious challenges as these can lead to acid mine drainage. Only a few local contractors use the waste materials, e.g. as fine aggregates for molding road curbs; the material is cheaply available. Despite this development, huge quantities of quarry wastes have remained unutilized resulting in serious environmental and economic problems because dusts can be dispersed easily by gravity, water, and wind. At present, no technological studies exist on the industrial applications of indurated shale-quarry waste (ISQW) in the ceramics industries in spite of several studies on Albian indurated shales, e.g. on their compositions (Cratchley & Jones, 1965; Akpokodje et al., 1991; Obiora & Charan, 2011), and on their use as construction aggregates (Nweke & Okogbue, 2021; Okogbue & Nweke, 2018). For economic reasons, the ceramics industry uses clayey materials from nearby deposits. The selection of appropriate raw materials is based on specific criteria which are related to the technological behavior during the various stages of manufacturing (El Ouahabi et al., 2014; Yongue-Fouateu et al., 2016) and the overall chemical composition (Diko-Makia & Ligege, 2020; Semiz & Çelik, 2020); the objective of the present study was to evaluate the mineralogy and the chemical, physical, and

**Fig. 1** Albian indurated shale from Abakaliki, southeastern Nigeria: **a** Agbaja active quarry, **b** lumps of crushed quarry rock, and **c** indurated-shale quarry waste materials from one of the quarries



https://doi.org/10.1007/s42860-023-00240-w Published online by Cambridge University Press

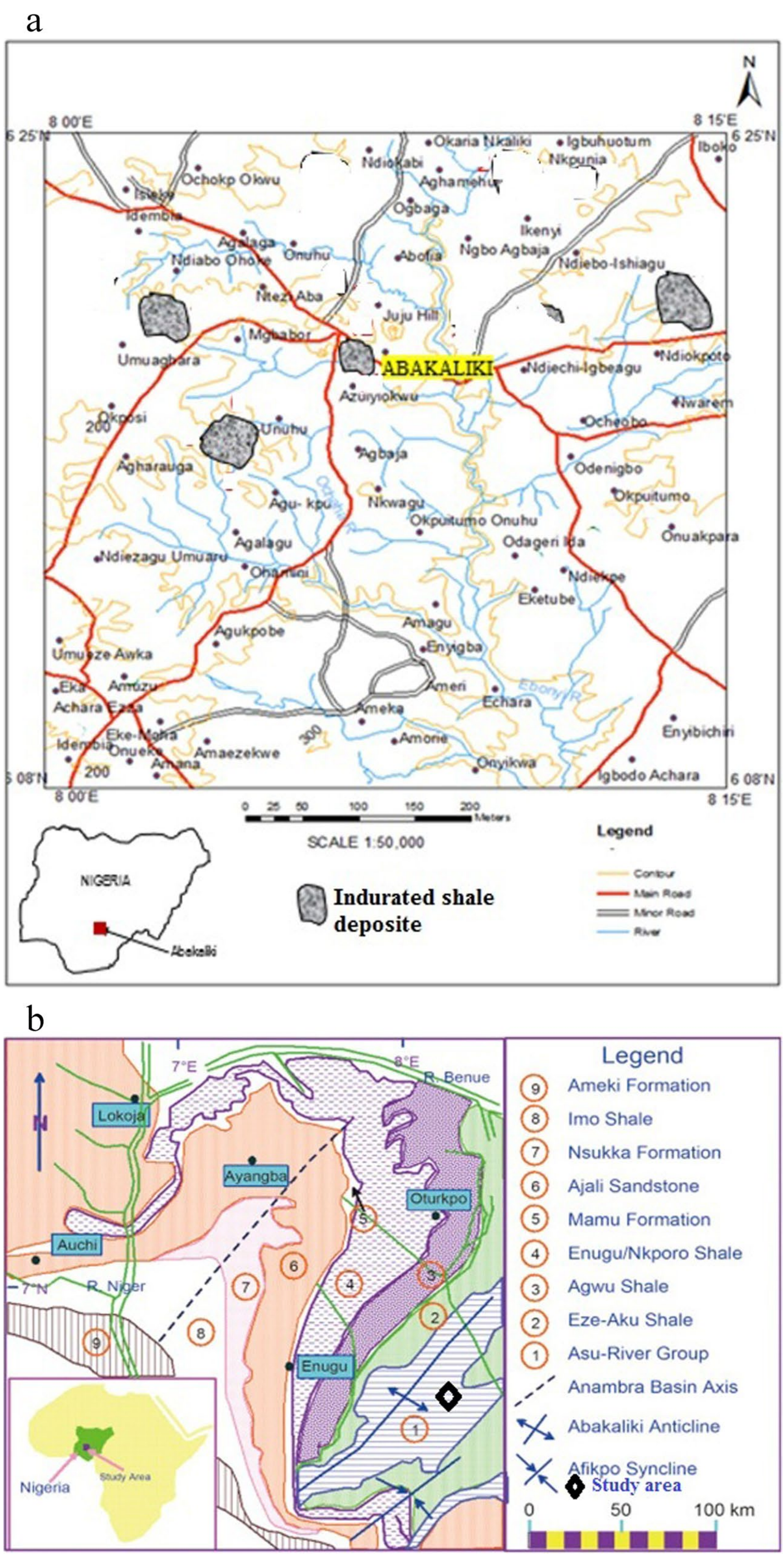




https://doi.org/10.1007/s42860-023-00240-w Published online by Cambridge University Press

◂**Fig. 2** **a** Map of Abakaliki and its environs showing the sample locations, **b** regional stratigraphic map of the southern Benue Trough, Nigeria (adapted from Nwajide, 1990) showing the Asu River Group where the study was carried out

technological properties of indurated shale-quarry wastes to establish their possible potential in the production of ceramics. Various diagrams, including those by Holtz and Kovacs (1981), McNally (1998), the Casagrande clay workability chart (Diko-Makia & Ligege, 2020), Winkler's (1954) diagram (Diko-Makia & Ligege, 2020), and a compositional ternary diagram (Diko-Makia & Ligege, 2020; Marsigli & Dondi, 1997), were employed to establish the suitability of ISQWs as potential raw materials in the ceramics (roofing tiles) industries. After studying the characteristics of the waste materials, the samples were fired (heat treated) from 800 to 1000°C and the technological properties of the fired product determined. The introduction of technological revolutions such as fast firing, according to Dondi et al. (2014) and Temga et al. (2019), will bring about drastic changes in raw materials and eventually give rise to novel products. The main scope of this research, therefore, hinged on the optimal exploitation of low-cost and locally available raw materials to reduce production costs and avoid limits on the production of roofing tiles necessary for socio-economic development as well as the creation of employment opportunities within the region.

## Geographical and Geological Setting

### Description of the Location and Physiology

The study area covers the Abakaliki metropolis (Fig. 2a) and its suburbs of Ezza North, Ebonyi, and the Abakaliki Local Government Areas of Ebonyi State. The area is located between the latitudes 06°15'N and 06°25'N north of the equator and longitudes 08°00'E and 08°10'E east of the Greenwich meridian, covering ~420 km$^2$. It has quite a good network of roads connecting the city center to the suburbs. The area can be accessed through a network of tarred roads including Abakaliki–Enugu, Abakaliki–Ishieke, and Abakaliki–Afikpo. The relief of the area exceeds 400 m above-sea-level in most locations such as the Azugwu, Umuoghara, and Sharon areas, all within the Abakaliki metropolis. Hills formed by pyroclastic bodies serve as the major relief structures while the low-lying areas are usually waterlogged during the rainy season and are predominantly underlain by shale. The Iyiokwu, Iyiudene, and Ebonyi Rivers are among the main rivers that drain the area along with a few minor drainage flows. The drainage systems flow eastward to join the Cross River in Cross River State which is outside the study area. Tropical rainforest, with distinct wet and dry seasons, is the typical vegetation in the area (Okogbue & Nweke, 2018). The dry season which lasts from November to March is characterized by a period of dry hot weather, while the rainy season which usually begins in April and ends in October is characterized by a prolonged period of rainfall with a short period of reduced rains in August. The average monthly rainfall ranges from 31 mm in January to 270 mm in July, with the dry season experiencing much reduced rainfall.

### Geology of the Indurated Shale of Southeastern Nigeria

Previous studies (Agumanu, 1989; Akande & Muche, 1989; Odoma et al., 2015; Reyment, 1965; Simpson, 1954) gave detailed accounts of the geology, stratigraphy, and economic potential of Abakaliki in the Lower Benue Trough, Nigeria. The tectonic history of the Lower Benue Trough was dated to pre-Albian time (Agumanu, 1989; Akande & Muche, 1989; Burke et al., 1971; Nwajide, 1990; Reyment, 1965; Simpson, 1954). The Abakaliki–Benue Trough (Fig. 2b) originated as a failed arm of the triple junction rift-ridge system during the break-up of Gondwana (Burke et al., 1971; Olade, 1979), which led to the separation of Africa from South America during the Aptian/Albian. Sedimentation in the Trough, according to Reyment (1965), was believed to have been initiated after the separation South America from Africa and was controlled by tectonic events and epeirogenic movement. The first marine transgression in the trough started in the mid-Albian period with the deposition of the Asu River Group (ARG) sediments. The ARG sediments were regarded as the oldest Cretaceous sediments in the basin and overlay unconformably on the Precambrian basement complex. The Asu River Group sediments consist mainly of olive-brown or bluish-gray shales and sandy shales, fine-grained micaceous sandstones, and micaceous mudstones with thin limestones around Abakaliki (Agumanu, 1989; Nwajide, 1990; Simpson, 1954); of dark gray–black pyritic micaceous shales, which in many cases were hardened or indurated by the effect of tectonism around Abakaliki with an average thickness of ~2000 m; and of thin sandstone and siltstone beds, magnetite and dolomitic horizons at Ngbo, with an estimated thickness of ~2500 m (Agumanu, 1989; Nwajide, 2013). In addition, Reyment (1965) and Benkhelil (1989) described the ARG sediments as consisting mainly of arkosic sandstones, volcaniclastics, marine shales, siltstones, and limestone. Previous authors (e.g. Cratchley & Jones, 1965; Obiora & Charan, 2011; Okogbue & Nweke, 2018) attributed the induration of the Albian calcareous shales deposited widely within the Abakaliki region to the effect of contact metamorphism during the igneous intrusion at pre-Santonian.

## Materials and Methods

### Sampling

The ISQW materials were obtained from the representative indurated shale bodies distributed widely across the Abakaliki region, southeastern Nigeria. The indurated shale bodies are currently quarried, crushed, and utilized as road and building construction aggregates in the Abakaliki metropolis and other neighboring states in southeastern Nigeria. The quarried waste samples from the five selected quarries were designated as ISQW1-Agbaja quarry, ISQW2-Umuoghara quarry, ISQW3-Abaofia quarry, ISQW4-Ezzangbo quarry, and ISQW5-Echara quarry. In each of the active quarries, full bags of bulk-rock samples were collected from at least two different points, for laboratory tests. The rock samples from the five locations showed no differences in color (Fig. 1), texture, or quality. The various bags full of samples were packaged in separate polyethylene sacks, labeled, and transported to the laboratory at the National Steel Raw Materials Exploration Agency in Kaduna, Nigeria, where sample preparation and laboratory testing on each of the samples commenced within 48 h of sampling. The samples were analyzed using various basic laboratory tests while specimen briquettes were molded for technological tests.

### Preparation and Laboratory Testing Methods

The standard procedures adopted for laboratory tests followed those specified in the American Society for Testing Materials standards (ASTM C326-09, ASTM C373, ASTM D-422, ASTM D4318, and ASTM C1167). The waste samples were ground into fine sizes (<2 μm size fraction using an agate mortar and dried in an oven at ~105°C for 24 h. The mineralogical analyses were carried out using X-ray diffraction (XRD) and the methodology adopted was in accordance with those adopted by Moore and Reynolds (1989) and Odoma et al. (2015). The analysis was performed using a PANalytical X'Pert Pro powder diffractometer equipped with an X'Celerator detector coupled with receiving slits, variable divergence and Fe-filtered Cu-Kα radiation ($\lambda = 1.7890$ Å). Qualitative X-ray diffraction analyses of the ISQW samples were carried out using a Bruker AXS D8 Advance PSD system operated at 40 kV and 40 mA, scanning between 3 and 85°2θ with a step size of 0.034°2θ and timing of 2 s/step with CuKα radiation. The silt and clay fractions were obtained by hydrometer analyses which were based on Stoke's Law of sedimentation of each individual particle falling at a constant velocity under gravity after the removal of carbonate by HCl (10%). After carbonate removal, clay was deflocculated by successive washings with demineralized water. The <2 μm fraction of the waste was separated by centrifugation. X-ray diffraction patterns were collected under three treatments (natural, ethylene glycolation, and heating at 500°C for 4 h) ranging from 2 to 70°2θ for bulk samples and from 2 to 40°2θ for samples which were air-dried, ethylene-glycolated for 24 h, and heated at 550°C for 4 h for the <2 μm size fraction. Sample ISQW1 was used as a representative sample due to similarities in texture, composition, and origin noted in the five samples. Mineral identification from the diffractogram and a semi-quantitative mineralogical composition were carried out using *EVA* software. The semi-quantitative abundances of the minerals identified in the ISQW samples were estimated from the height of diagnostics peaks multiplied by their respective corrective factors (Boski et al., 1998; Brindley, 1980; Cook et al., 1975; Fagel et al., 2003). X-ray fluorescence (XRF) spectrometry was used to determine the oxide % of



https://doi.org/10.1007/s42860-023-00240-w Published online by Cambridge University Press

elements on the < 2 μm size fraction of the ISQW samples. The XRF tests followed the standard procedures described by Viani et al. (2018) and Nweke and Okogbue (2021). The Philips PW 1600 X-ray fluorescence spectrometer (Malvern Panalytical Ltd., Malvern, UK) equipped with an end-window 4 kW Rh-anode X-ray tube was used. The energy-dispersive XRF system was made up of an excitation source, sample chamber, silicon (lithium) drift detector, signal processing and recording system (preamplifier), multichannel analyzer, and video display unit. The ISQW samples were crushed into powdered form in a tungsten crushing vessel and ~6.25 g of the powdered waste samples were mixed with ~1.4 g of wax (M-HWC); in order to obtain a pressed disc, the mixtures were compressed using a force of 18 N. The dilution factor (0.8169) was calculated from the mass of the ISQW samples and total dilution mass. The total organic matter of the waste samples were determined by Loss on Ignition (LOI) determined at 500°C for 4 h (Heiri et al., 2001; Semiz, 2017). The grain-size distribution analyses of the samples were performed by wet sieving for particles which are ≥ 80 μm and by sedimentometry for particles which are ≤ 80 μm in accordance with the ASTM D-422 (1972) standard. The fines fractions of the waste samples were characterized using hydrometer analysis based on Stoke's law of sedimentation. The degree of plasticity of the samples was achieved via the Atterberg limits (liquid limit, LL and plastic limit, PL) using the Casagrande apparatus in accordance with the ASTM-D4318 (2010) standard described by Casagrande (1947) and Nweke and Okogbue (2021). The Atterberg limits tests were carried out using ~100 g of air-dried soils passing a 0.425 mm sieve (a No 36 British Standard BS International sieve) following the standard procedures as specified by ASTM-D 4318 (2010) and British Standard 1377 (BS, 1990). The plasticity index (PI) for each of the ISQW samples was obtained from the difference between LL and PL whereas the clay activity (CA) was calculated using Eq. 1

$$CA = PI/clay wt.\% \tag{1}$$

In order to study the evolution of firing properties of the ISQW samples, cylindrical ISQW samples were prepared. The ISQW samples were oven dried at 105°C for 24 h and ground to a fine powder, then sieved using a mesh-size of 100 μm and were mixed with 26–28% water content to enhance particle binding in order to produce a cylindrical shape. Then the wetted powdered ISQW samples were pressed under 1500 N pressure to obtain 100 mm × 50 mm × 8 mm prismatic samples. Then the samples were air dried for 24 h and oven dried at 105°C for 24 h to ensure that absorbed moisture was eliminated. After drying, the specimens were cooled in a drying room maintained at a temperature of 24°C, with a relative humidity of between 30 and 70%. Thereafter, the specimens were stored in the drying room at the required temperature of 105°C and humidity of 70% until they were tested. Using a laboratory kiln, the dried ISQW samples were fired at 800, 900, and 1000°C (in 100°C intervals) for 5 h at a heating rate of 5°C/min using an electrically powered laboratory furnace. Fired samples were used for characterization of the raw materials according to the standards suggested by the ISO10545-3 method. The raw materials were subjected to heat treatment (high-temperature firing) of 1000°C in order to provide the required strength and durability. The fired ISQW specimens were tested for ceramics properties such as linear shrinkage, weight loss, bulk density, water absorption, and flexural strength as part of the ceramics evaluation and the various technological tests were conducted in accordance with standards such as: IS 3495–2, ASTM C373-14 (2014), ASTM C326-09 (2009), and ASTM C1167 11 (2017). Four tests were conducted for each property and the average results were tabulated.

The linear shrinkage (LS) of the studied ISQW was calculated using Eq. 2

$$LS(\%) = [(L_0 - L)/L_0] \times 100 \tag{2}$$

This expression depends on the relative variation length of the briquette, where $L_0$ represents the length of the briquette before firing and $L$ represents the briquette after firing.

The water absorption capacity (WA) of the ISQW was measured by weighing the fired briquette ($M_1$) and the wet briquette ($M_2$) after immersion in water for 24 h and was indicated with an expression as follows:



https://doi.org/10.1007/s42860-023-00240-w Published online by Cambridge University Press

$$WA(\%) = \left[M_2 - M_1)/M_1\right] \times 100 \quad (3)$$

The weight loss (WL) of the ISQW studied was calculated as follows:

$$WL(\%) = \left[\left(M_{d^-} - M_f\right)/M_d\right] \times 100 \quad (4)$$

where $M_d$ represents the dry mass (g) at 105°C and $M_f$ represents the fired mass (g) at each final firing temperature.

The bulk density (BD) of the ISQW briquette is represented in Eq. 5 as:

$$BD\,(g/cm^3) = M_f/V \quad (5)$$

where $M_f$ is the fired briquette weight (g) and $V$ represents the measured volume ($cm^3$) of the briquette.

The flexural strength (FS) of the ISQW samples studied was evaluated using the three-point bending-test method in accordance with the ASTM F417-96 procedure described by Yongue-Fouateu et al. (2016). The value of modulus of FS for each specimen was computed and recorded to the nearest 0.01 MPa with the expression represented as follows:

$$FS\,(MPa) = 3FL/2bd^2 \quad (6)$$

where $F$ = maximum load, $L$ = distance between the supports (mm), $b$ = net width of the specimen at the plane of failure (mm), and $d$ = depth of the specimen at the plane of failure (mm).

## Results and Discussion

### Mineralogical and Chemical Characteristics of Indurated Shale

Representative matched XRD patterns for all of the minerals identified in one of the ISQW materials studied (ISQW 1 sample) are presented in Fig. 3a. The remaining matched XRD patterns are given in the Supplementary Material file. The prominent peaks at 25.4, 26.5, 27.6, and 35.6°2θ (2.5 and 3.4 Å) are characteristics of quartz. Other characteristic peaks of quartz include 4.25 and 3.34 Å. Chlorite minerals were identified by the persistence of the second reflection at ($d$ = 7.0 and 14 Å) during heating and feldspars were identified at $d$ = 3.19 and 3.24 Å. Peaks observed at 3.51, 4.15, 2.71, and 10.01 Å were assigned to anatase, goethite, hematite, and muscovite, respectively. The results, however, revealed the predominance of clay minerals (illite-kaolinite-smectite-vermiculite) (48.4%), with large quartz contents (30%) along with considerable amounts of carbonate and feldspar as well as jarosite, rutile, anatase (16.6%). The intensities of peaks characterizing each clay mineral present in the size fraction were measured for a semi-quantitative estimate of the proportion of clay minerals present in the < 2 μm size fraction (untreated, ethylene glycolated for 24 h, and heated at 550°C). From the semi-quantitative abundance of the minerals identified in the representative ISQW sample, the mineralogical composition of the indurated shale as illustrated in Fig. 3b was summarized in Table 1. According to Moore and Reynolds (1989), Rieder et al. (1998), and Murray (2007), the mineralogical components refer to the relative abundance and identification of the clay minerals. The presence of aluminosilicates (Rieder et al., 1998) such as illites (group of closely related non-expanding clay minerals) in each of the tested ISQW samples were indicated by the visible peak intensities at $d$ = 10 Å. Characteristic peaks of kaolinites were identified at 7.13, 4.36, 4.16, and 3.57 Å whereas smectites were indicated by their characteristic peak at 14 Å under natural conditions, which migrated to 16 Å after glycolation and later collapsed to 10 Å after heating. Brindley and Brown (1980) and Rieder et al. (1998) had earlier described illites as clay-size mica, a dioctahedral mineral found in 2:1 clay minerals with non-expandable layers; they are common in sediments, argillaceous rocks, and in low-grade metamorphic rocks. Previous researchers (Agumanu, 1989; Akpokodje et al., 1991; Nweke & Okogbue, 2021), revealed that the Albian shales of the Asu River Group sediments were dominated by illite with smectite, chlorite, and kaolinite as found as minor components while quartz, feldspar, and carbonate were regarded as the main non-clay minerals. A small quartz content in the raw materials usually reduces the strength of the ceramics specimen (Zeballos et al., 2016), which affects adversely the quality of the end product. This is not likely to be the case with ISQW considering the amounts of quartz (generally ≥ 30%) in each tested sample. Feldspars are regarded as the source of both the alkali content and the alumina needed in the fine ceramics industry as a flux in the formation of glassy phases which promote vitrification and translucency



https://doi.org/10.1007/s42860-023-00240-w Published online by Cambridge University Press

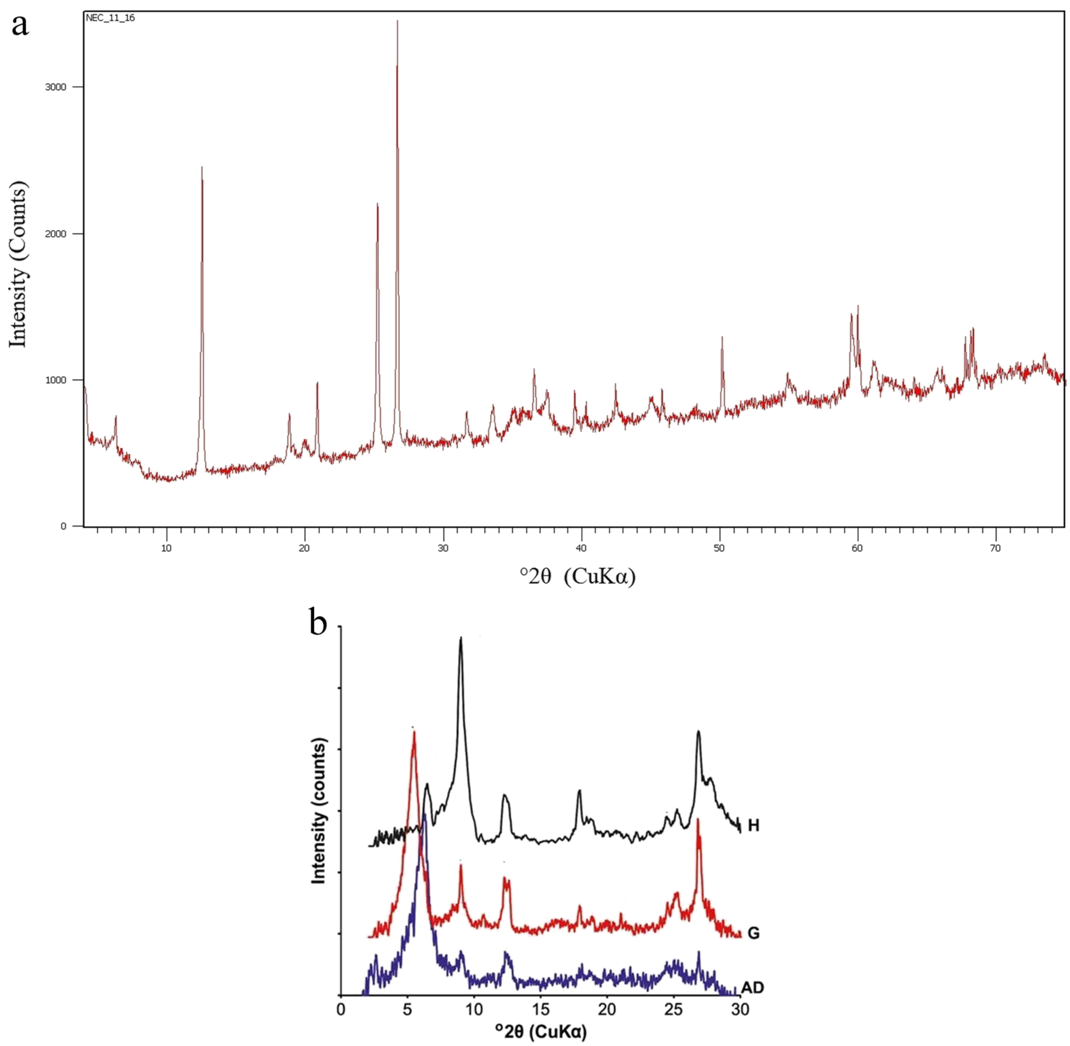


**Fig. 3** **a** XRD analysis of the ISQW from Abakaliki, southeastern Nigeria, **b** clay fraction of representative ISQW samples. Illite dominated in the left-hand patterns. Normal (H), glycolated (G), and heated at 550°C (AD)

(Moharem & Saleh, 2007; Lori, 2008). The feldspar in the present study may also serve as a vitrifying (fluxing) agent that can form a glassy phase at intermediate temperature which will probably guarantee better fusibility for the raw material in the production of roofing tiles. The amounts of smectite (<10%) are considered to be very small; an indication of the small likelihood of the ISQW samples cracking or shrinking especially during drying or firing. This was regarded as an advantage in terms of tile manufacture. Although chlorite minerals were found in all of the ISQW samples tested, they are usually eliminated in

**Table 1** Mineralogical composition (wt.%) of the representative sample of the Albian-indurated shale

| Whole rock | | | | | | <0. 002 mm fraction | | | | |
|---|---|---|---|---|---|---|---|---|---|---|
| Sample ID | Quartz | Feldspar | Carbonate | Chlorite | Clay | Kaolinite | Smectite | Illite | Chlorite | Vermiculite |
| ISQW | 30 | 7.5 | 9.1 | 4.9 | 48.4 | 10.2 | 5.3 | 74.0 | 9.4 | 1.4 |



https://doi.org/10.1007/s42860-023-00240-w Published online by Cambridge University Press

the sintering process and as such, their presence is not often considered to be a serious problem. To understand better the mineralogy of the indurated shales, the ternary composition diagram used by Strazzera et al. (1997) for ceramic raw materials from southern Sardinia (Italy) was adapted here. Using the ternary compositional diagram based mainly on the total clay mineral-carbonate-quartz + feldspar diagram (Fig. 4a), the mineralogical classification of the ISQW revealed that the representative ISQW sample tested fell within roofing-tile region.

The chemical compositions of the ISQW samples were investigated by XRF analysis and the results as presented in Table 2 revealed the presence of major oxides with various amounts of $SiO_2$ (57.1–60.1%) > $Al_2O_3$ (16.7–17.8%) > CaO (4.30–6.20%) > $K_2O$ (4.05–6.05%) > $Fe_2O_3$ (1.94–3.39%), > $Na_2O$ (0.93–1.36%). Most importantly, chemical analyses allowed for rapid classification of raw materials for optimal ceramics applications. In the manufacture of roofing tiles, the chemical composition of raw materials, according to Diko-Makia and Ligege (2020) is regarded as an important factor and is related to the mineralogy, especially to the amount of quartz and type of clay minerals present. The concentrations of $SiO_2$, $Al_2O_3$, and $K_2O$ in each of the rock samples meant that they were dominated by quartz and illite as the non-clay mineral and clay mineral, respectively. The values of $SiO_2$ and $Al_2O_3$ were observed to be close to those of the plastic fire clay of St. Louis, Missouri (Huber, 1985), which had an $SiO_2$ value of 57.6% and an $Al_2O_3$ value of 24.0%. According to Pontikes et al. (2007), large amounts of $Al_2O_3$ in

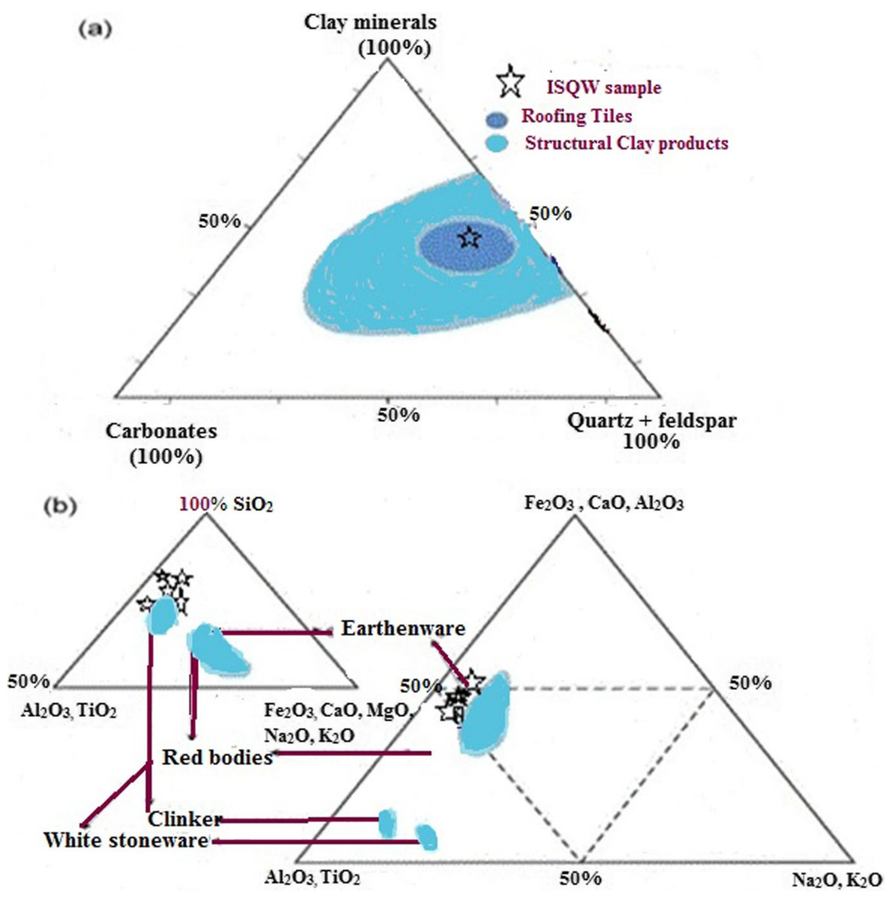


**Fig. 4** Mineralogical and chemical classification of raw materials based on: **a** clay minerals, carbonate, and quartz + feldspar ternary diagram (Diko-Makia & Ligege, 2020); **b** major oxide contents showing ISQW utilization (adapted from Akintola et al., 2020; Diko-Makia & Ligege, 2020)

**Table 2** Results of the chemical analysis (wt.%) of the Albian-indurated shale

| Sample Code | $SiO_2$ | $Al_2O_3$ | $SO_3$ | $Na_2O$ | $K_2O$ | CaO | MgO | $TiO_2$ | $Fe_2O_3$ | MnO | LOI | Total | $SiO_2$/ $Al_2O_3$ | Calculations | | | | |
|---|---|---|---|---|---|---|---|---|---|---|---|---|---|---|---|---|---|---|
| | | | | | | | | | | | | | | 1 | 2 | 3 | 4 | 5 |
| ISQW 1 | 60.1 | 17.8 | 0.04 | 1.36 | 5.05 | 5.2 | 0.48 | 0.75 | 1.94 | 0.09 | 7.21 | 99.2 | 3.38 | 6.4 | 5.68 | 18.6 | 7.6 | 14.0 |
| ISQW 2 | 59.0 | 16.7 | 0.32 | 1.30 | 5.09 | 6.2 | 0.50 | 0.76 | 3.39 | 0.11 | 6.43 | 100.1 | 3.53 | 6.4 | 6.70 | 17.5 | 10 | 16.4 |
| ISQW 3 | 58.1 | 17.2 | 0.80 | 0.93 | 4.05 | 4.3 | 0.48 | 0.72 | 2.60 | 0.09 | 10.4 | 99.97 | 3.38 | 4.9 | 4.78 | 17.9 | 7.4 | 12.3 |
| ISQW 4 | 57.1 | 17.3 | 0.90 | 1.36 | 6.05 | 5.2 | 0.48 | 1.75 | 2.94 | 0.09 | 7.01 | 99.2 | 3.30 | 7.4 | 5.68 | 19.1 | 8.6 | 16.0 |
| ISQW 5 | 59.7 | 16.7 | 0.87 | 1.30 | 5.09 | 5.2 | 0.50 | 1.76 | 2.39 | 0.11 | 6.43 | 99.1 | 3.57 | 6.4 | 5.70 | 18.5 | 8.1 | 14.5 |
| Min | 57.1 | 16.7 | 0.04 | 0.93 | 4.05 | 4.3 | 0.48 | 0.75 | 1.94 | 0.09 | 6.43 | | | | | | 7.4 | 12.3 |
| Max | 60.1 | 17.8 | 0.90 | 1.36 | 6.05 | 6.2 | 0.50 | 1.76 | 3.39 | 0.11 | 10.4 | | | | | | 10 | 16.4 |

LOI = Loss on Ignition

1 = $Na_2O + K_2O$

2 = $CaO + MgO$

3 = $Al_2O_3 + TiO_2$

4 = $CaO + MgO + Fe_2O_3$

5 = $CaO + MgO + Fe_2O_3 + Na_2O + K_2O$



https://doi.org/10.1007/s42860-023-00240-w Published online by Cambridge University Press

raw materials often help in improving the strength and hardness of the final ceramics product. The large amounts of $Al_2O_3$ (16.7–17.8%) in the ISQW materials which suggested a bauxitic composition from which kaolinitic minerals might have ensued, correspond to refractory industrial specifications (Parker, 1967) and ceramics products (Singer & Sonja, 1971). The $SiO_2$:$Al_2O_3$ ratios of the indurated shales ranging from 3.38 to 3.57 are noted to be greater than the values found in pure kaolinite ($SiO_2$:$Al_2O_3$ = 1.18) and smectite ($SiO_2$:$Al_2O_3$ = 2.36), a situation related partly to the amount of free silica (quartz) (Tsozue et al., 2017; Semiz and Çelik, 2020), suggesting the excess $SiO_2$ which was represented in > 52% of the samples tested. The $SiO_2$:$Al_2O_3$ molar ratio usually ranges between 1.6 and 2.6 in the plastic fire clay, between 2.4 and 4.0 in ball clay, and between 3.5 and 6.7 in siliceous fire clay (Baioumy & Ismael, 2014; Temga et al., 2019). The CaO concentrations (4.3–6.20%) were variable and related to carbonate contents (7.2–10.5%), according to the XRD analyses. The relatively large $K_2O$ values reflected the predominance of illite in the indurated shale rock of Asu River Group sediments (Akpokodje et al., 1991; Nweke & Okogbue, 2021). According to Galan (2003), $Na_2O$ and $K_2O$ are regarded as essential in the production of roofing tiles because they act as fluxing agents, thereby reducing the melting points of ceramic mixtures. The fluxing agents such as alkali oxide ($Na_2O$ and $K_2O$; 4.98–7.41%) and alkaline earth oxides (CaO and MgO; 4.78–6.70%) were noted to be generally > 4.0%, an indication of possible densification of ISQW at high temperature. Carbonate-rich raw materials yield light-colored products (Peters & Iberg, 1978). According to Rooney (1984), Bun Kim et al. (2011), and Daoudi et al. (2014), the $Fe_2O_3$ contents are often sensitive to firing conditions as they can produce unexpected results in terms of the color and texture of the fired clays. High concentrations of $Fe_2O_3$ are not acceptable for use in ceramic manufacture because light colors are required. According to Dondi et al. (2002) and Semiz and Çelik (2020), classifications based on $Fe_2O_3$ concentrations of clay-rich raw materials are as follows: (1) red firing clays, $Fe_2O_3$ concentration > 5%; (2) tan burning clays, $Fe_2O_3$ concentration between 1 and 5%; and (3) white firing clays, $Fe_2O_3$ concentration < 1%. The $Fe_2O_3$ concentrations of the ISQW materials studied (1.94–3.39%) fell within the class of tan burning clay material. However, the concentration of $Fe_2O_3$ was not regarded as the main factor related to coloration of ceramic products. The presence of $TiO_2$ along with $Fe_2O_3$, according to Diko-Makia and Ligege (2020) and Oyebanjo et al. (2020), can be associated with discoloring components such as hematite, goethite (Fe-hydroxide), and anatase. Keller (1968) and Oyebanjo et al. (2020) further described raw materials containing $TiO_2$ ranging from 1 to 3 wt.% and $Fe_2O_3$ with values ≥ 3.0 wt.% as being of no use to the ceramist because such concentrations are considered undesirable, especially for roofing-tile manufacture (Zeballos et al., 2016). The concentrations of MgO (0.48–0.50%), $TiO_2$ (0.75–1.76%), and $Fe_2O_3$ (1.94–3.39%) here are well within the acceptable limit, and probably won't have a negative impact on the color of the final ceramic product. The small and similar values in the $Fe_2O_3$ contents reflected homogeneous stability in terms of tonality and color which can favor white ceramic formulations. $SO_3$ is another harmful oxide for ceramic materials (Terrones-Saeta et al., 2020) but in the case of the ISQW samples studied, the $SO_3$ values ranging from 0.04 to 0.9% are considered small. The LOI values (6.43–10.4%) can be attributed to the dehydroxylation of clay minerals, organic matter oxidation, and decomposition of carbonates and hydroxides (Celik, 2010; Semiz, 2017). As specifications for the industrial applications relate to the major oxides, Fig. 4b depicts the chemical data on a ternary diagram ($Fe_2O_3$ + CaO + MgO)/$Al_2O_3$/($Na_2O$ + $K_2O$) used by Fiori et al. (1989) to classify raw clay materials and industrial ceramic bodies and those of the studied ISQW materials showed that they have oxide values very close to outliers for earthenware and red clay body production as well as clinker and white stoneware. The alkali and alkaline earth elements (CaO + MgO + $Fe_2O_3$ + $Na_2O$ + $K_2O$; 12.3–16.4%) in addition to the presence of illite and feldspar might guarantee a good fusibility for ceramic production (Akintola et al., 2020; Tsozue et al., 2017). The amounts of fluxing oxides in the ISQW samples will allow for sufficient sintering during firing to guarantee the formation of vitreous phases. Sintering temperature is often an important processing variable which can influence significantly the final ceramic product (Serra et al., 2013; Diko-Makia & Ligege, 2020) and poor vitreous-phase formation usually influenced negatively the cohesion of the products fired (Onana et al., 2019). Based on



https://doi.org/10.1007/s42860-023-00240-w Published online by Cambridge University Press

chemical specifications, the concentrations of $SiO_2$, $Al_2O_3$, MgO, and $Fe_2O_3$ are within the allowable international parameters for ceramics formulations. The ISQW materials are rich in $SiO_2$ and $Al_2O_3$ which have great influence in terms of the development of ceramic materials.

Physical Characteristics of Indurated Shale

The results of the grain-size distribution tests conducted on the ISQW samples are presented in Table 3. The International Society of Soil Science classifies soil according to its dimension and was subdivided into clay, silt, and sand fractions. From Table 3, the clay fraction ranged from 22 to 28%, the silt fraction ranged from 42 to 48% while the sand fraction ranged from 24 to 38%; an indication of the predominance of clay-silt materials. Grain-size distribution has fundamental importance in the characterization of raw materials for traditional ceramics applications (Akintola et al., 2020). It can indicate the plastic behavior and firing behavior exhibited by the raw material, as well as the mechanical strength of the fired product. It also controls to a significant extent the technological parameters during the drying and firing processes as sands are predictably reactive upon firing especially at lower temperatures (Akintola et al., 2020). For ceramics products, the <2 μm fraction is of particular importance (Mahmoudi 2008). Large proportions of the <2 μm fraction (i.e. >80% of the total), according to McNally (1998) and Ekosse (2010), will account for excessive shrinkage during firing; this is not likely be the case for the ISQW samples. The amount of <2 μm fractions (22–28%) obtained can result in very limited cracking due to shrinkage when fired for ceramics applications. The clay fraction may, therefore, be regarded as an added advantage in confirming the suitability of the raw material for roofing-tile fabrication. The sand fraction (24–38%) present in the ISQW also has a significant role to play in the technological behavior. To formulate roofing-tiles ceramics bodies, a Winkler Diagram was used to obtain products with good technological properties (Diko-Makia & Ligege, 2020; Semiz, 2017; Winkler, 1954; Yongue-Fouateu et al., 2016). Raw materials are usually plotted on a Winkler diagram (Fig. 5a) in order to evaluate their suitability for various ceramics products which included: (1) common bricks, (2) vertical perforated/corrugated bricks, (3) roofing tiles/wall tiles, and (4) perforated or hollow products. From the Winkler diagram (Fig. 5a), the ISQW samples matched most closely the vertical corrugated bricks and roofing tiles. The raw materials were further plotted on the proposed McNally diagram (Fig. 5b) for brick and tile production. From the diagram, three samples plotted within the region of roofing tiles while the other two samples plotted between the perforated bricks region, indicating that they are unsuitable materials (due to their liability to excess shrinkage on firing).

The results of the Atterberg limits tests of the ISQW materials studied as presented in Table 3 revealed that the LL ranges from 44 to 50%, the PL ranges from 16 to 27% while the PI ranges from 21 to 34%. In the application of clay materials in the ceramics industries, plasticity is considered an important parameter which assists in determining the clay

**Table 3** Results of the grain-size distribution and Atterberg limit tests of indurated shale-quarry waste samples

| S/N | Quarry Location | Sample ID | Grain-size distribution | | | Atterberg limit | | | |
|---|---|---|---|---|---|---|---|---|---|
| | | | Clay (%) <2 μm | Silt (%) 20–2 μm | Sand (%) >20 μm | LL (%) | PL (%) | PI (%) | Clay Activity (%) |
| 1 | Agbaja | ISQW 1 | 24 | 48 | 28 | 44 | 16 | 28 | 1.17 |
| 2 | Umuoghara | ISQW 2 | 28 | 46 | 24 | 50 | 16 | 34 | 1.21 |
| 3 | Abaofia | ISQW 3 | 26 | 44 | 30 | 47 | 26 | 21 | 0.80 |
| 4 | Ezzangbo | ISQW 4 | 20 | 42 | 38 | 48 | 27 | 21 | 1.05 |
| 5 | Echara | ISQW 5 | 22 | 48 | 30 | 46 | 18 | 28 | 1.27 |
| | Min | | 22 | 42 | 24 | 44 | 16 | 21 | 0.80 |
| | Max | | 28 | 48 | 38 | 50 | 27 | 34 | 1.27 |



https://doi.org/10.1007/s42860-023-00240-w Published online by Cambridge University Press

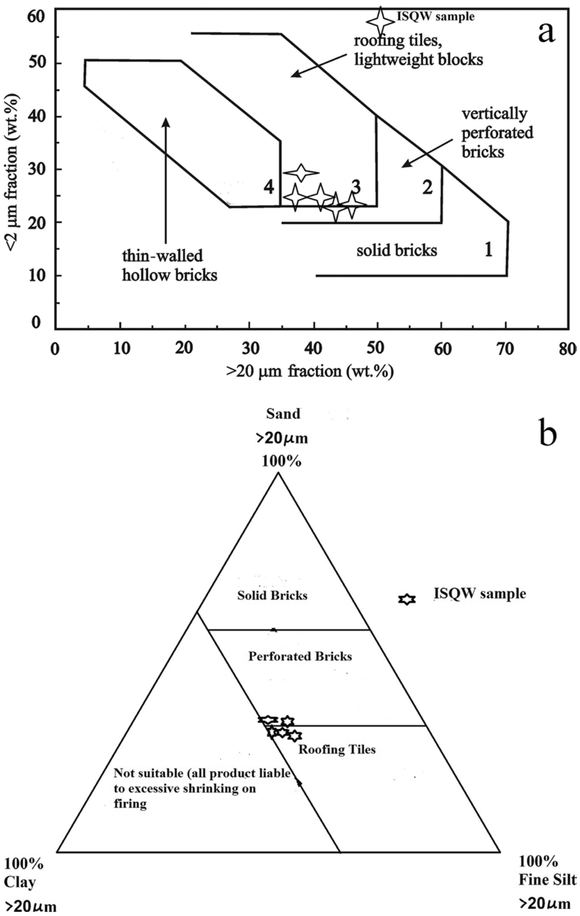


**Fig. 5** Grain-size distribution classification based on: **a** Winkler diagram for the technological classification of clay products (Winkler, 1954) and Diko-Makia & Ligege (2020). Fields are defined as: (1) common bricks, (2) vertically perforated/corrugated bricks, (3) roofing tiles and masonry bricks, and (4) perforated/hollow products, and **b** McNally diagram for raw material used in the production of bricks and tiles (adapted from McNally, 1998)

workability, drying behavior, and ceramic applications (Diko et al., 2011; Murray, 2007). The plasticity of clayey materials is controlled by factors such as grain-size distribution, mineralogy (especially the clay mineral in the raw material), and the presence of organic matter (Holtz & Kovacs, 1981; Daoudi et al., 2014). As shown in Table 3, the LL values (44–50%) agree with the range defined by other researchers, such as Baccour et al. (2009) and Semiz and Çelik (2020) (30–60%), in terms of the composition of raw materials used for ceramics production. The LL and PI values for the ISQW samples plotted on the Holtz and Kovacs (1981) diagram (Fig. 6a) revealed that all the tested ISQW samples plotted in the medium- to high-plasticity region. From the diagram, the medium plasticity displayed by the samples was consistent with the predominant clay mineral being illite (Bain, 1971). The scattered plots in the Holtz and Kovacs diagram which revealed that the raw materials fall within the illite and smectite region with medium plasticity, can be attributed to the abundance of fine and silt fractions. Generally, large clay and silt fractions usually give rise to relatively high plasticity. The large clay and silt fractions recorded (Table 3) and the smectite contents in the ISQW samples studied (Table 1) may be responsible for the relatively high plasticity, an indication of material with significant potential for swelling (Oyebanjo et al., 2020). Raw materials with PI values of between 7 and 10 have low plasticity and are not considered appropriate for use in building-related ceramics production as they would require addition of polymer in order to obtain adequate plastic behavior to avoid cracking during extrusion (Bain, 1971; Dondi et al., 2002; Oyebanjo et al., 2020). This is probably not the case with the quarry wastes studied as the PI values obtained were generally ≥20%. The minimum percentage of moisture required to obtain the necessary plasticity is defined by the PL parameter which is very important for the technological process in terms of drying (Monterio & Vieira, 2004). For any raw material it is important to note that PL ranging from 26 to 32%, according to Teixera et al. (2001), usually allows ceramics processing and/or conforming via the extrusion process.

According to Skempton (1953), the degree of colloidal activity is expressed by the ratio of PI to the percentage of the soil fraction which is <2 μm. That author suggested three classes of clays based on their activity, namely the inactive clays with activity values of <0.75, normal clays with activity values ranging between 0.75 and 1.25, and the active clays with activity values >1.25. In the current study, the clay activity (CA) obtained from the ISQW samples ranging from 0.80 to 1.27 were generally >0.75; a value which Skempton and Northey (1952) and Skempton (1953) considered normal to active; confirming the predominance of illitic clay minerals. Illite, according to Tsozue et al. (2017), is considered a special mineral that improves the plasticity of raw materials, favoring the occurrence of vitreous phases during



https://doi.org/10.1007/s42860-023-00240-w Published online by Cambridge University Press

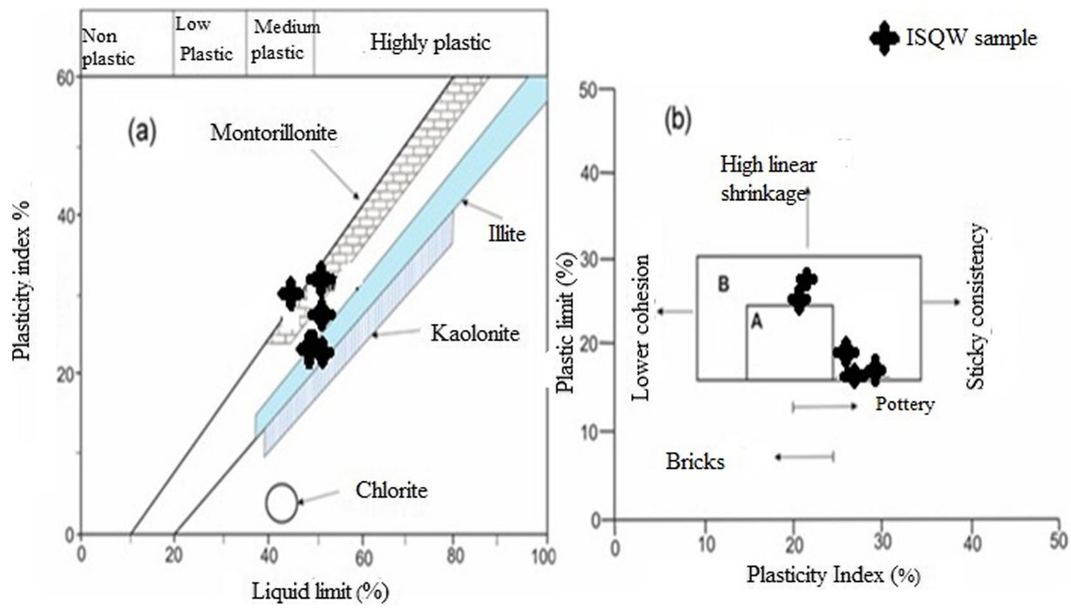


**Fig. 6** Atterberg limits of the indurated-shale quarry waste: **a** according to the Holtz and Kovacs (1981) diagram, **b** according to the Casagrande (1947) clay workability chart

firing, thereby improving densification and strength of the ceramic bodies. The proportions of illite which are considered large in the ISQW samples tested (see Table 1) would probably impact on the drying behavior and fired strength of the finished product. The Casagrande clay workability chart (Fig. 6b) revealed that the ISQW samples are generally of medium plasticity and suitable for ceramics production with significant linear shrinkage.

## Ceramics Properties of Indurated Shale-Quarry Waste

After drying for 24 h the ISQW samples were heated and various technological properties determined; the results are summarized in Table 4. According to ASTM C1167-11 (2017), heat treatment at elevated temperature is expected to assist development of a fired bond between material particles that can provide the required strength and durability. The results generated from the linear shrinkage (LS) tests (Table 4) indicated that the LS for each of the fired samples increased as the firing temperature increased. From the results, at an elevated temperature of 800°C, the linear shrinkage varied from 9.23 to 12.2% while at 1000°C, the LS varied from 14.8 to 18.3%, an indication of increment with heat treatment (Fig. 7). Shrinkage by drying and firing, according to Zeballos et al. (2016), is related directly to the amount and types of clay minerals as well as the physical water present in the plastic clay materials. The level of shrinkage observed in the fired materials can be argued to be consistent with the proportion of clay fraction present (Table 3). The increase in LS can be attributed to the breakdown of the clayey structure at high temperature (1000°C) which marked the beginning of the vitreous phases and the possible occurrence of the thermal decomposition of carbonates (El Ouahabi et al., 2014). The large quartz contents (Table 1) present in the extruded ISQW samples can also be responsible for the level of shrinkage of the samples. El Ouahabi et al. (2014) attributed the behavior exhibited by the ISQW samples during firing to the transition of alpha to beta quartz at higher temperature. The relatively high linear shrinkage was in agreement with the amount of smectite which can limit its application to produce tiles. This is due to the minimal shrinkage during firing of the raw material in ceramics processing, which is vital according to Garcia-Valles et al. (2020) and Oyebanjo et al. (2020). Linear shrinkage, according to Semiz and Çelik (2020), gives an indication of the efficiency of



https://doi.org/10.1007/s42860-023-00240-w Published online by Cambridge University Press

**Table 4** Results of technological tests conducted on Albian-indurated shale-quarry waste at various temperatures

| Sample Code | Fired Temperature | Linear shrinkage (%) | Water absorption (%) | Bulk density (g/cm$^3$) | Weight loss (%) | Flexural strength (MPa) |
|---|---|---|---|---|---|---|
| ISQW 1 | 800°C | 9.23 | 14.4 | 2.01 | 5.2 | 2.45 |
| | 900°C | 12.7 | 12.7 | 2.09 | 6.2 | 2.61 |
| | 1000°C | 17.8 | 9.80 | 2.19 | 8.3 | 3.22 |
| ISQW 2 | 800°C | 12.2 | 16.0 | 1.89 | 5.0 | 2.99 |
| | 900°C | 14.7 | 12.7 | 1.98 | 6.2 | 3.09 |
| | 1000°C | 18.3 | 10.6 | 2.00 | 7.3 | 3.21 |
| ISQW 3 | 800°C | 9.28 | 14.9 | 2.13 | 4.9 | 2.40 |
| | 900°C | 12.1 | 12.9 | 2.13 | 6.2 | 2.89 |
| | 1000°C | 14.8 | 9.12 | 2.23 | 6.3 | 3.23 |
| ISQW 4 | 800°C | 10.2 | 12.4 | 2.00 | 5.0 | 2.59 |
| | 900°C | 14.7 | 10.3 | 2.02 | 6.2 | 2.99 |
| | 1000°C | 15.3 | 8.33 | 2.20 | 7.3 | 3.31 |
| ISQW 5 | 800°C | 9.75 | 15.4 | 1.91 | 5.0 | 2.56 |
| | 900°C | 12.7 | 12.3 | 2.14 | 6.4 | 2.89 |
| | 1000°C | 16.8 | 10.7 | 2.18 | 8.5 | 3.99 |

firing, and the internationally acceptable LS values for aluminum silicates, kaolin, and fired clays ranging from 7 to 10% (Diko-Makia & Ligege, 2020; Manukaji, 2013). The LS values obtained in the current study ranged from 14.8 to 18.3% and were not within the internationally acceptable range of 7 (Manukaji, 2013; Semiz, 2017; Yongue-Fouateu et al., 2016) for possible use as raw materials in ceramics production.

The water absorption (WA) tests as carried out on the ISQW specimens indicated that at 800°C the WA varied from 12.4 to 15.4% while at an elevated firing temperature of 1000°C, the WA varied from 8.33 to 10.7%. The WA test usually reflects the water-retention

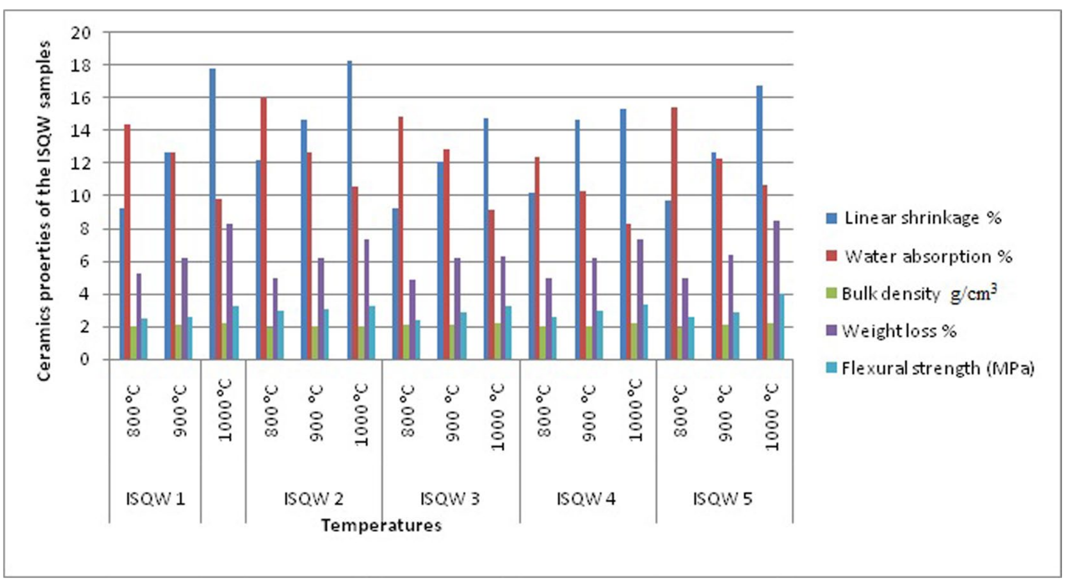


**Fig. 7** Firing behavior (heat treatment) of some technological properties as the fired temperature increased



https://doi.org/10.1007/s42860-023-00240-w Published online by Cambridge University Press

capacity of each of the samples. From the results, the WA capacity of the ISQW samples decreased significantly as the firing temperature increased (Fig. 7). The decrease in the WA for the fired ISQW could be translated to the dehydration reactions, decarbonation, and combustion of organic matter (Monterio & Vieira, 2004; Ngun et al., 2011) which influenced greatly the mechanical properties and durability of the raw materials thereby transforming them into more resistant and more durable materials. The decrease in the WA has been attributed (Kagonbe et al., 2021; Lambercy, 1993) to the formation of a glassy phase that penetrated the pores, closing them and isolating them from the neighboring pores. In ceramics specifications according to the ISO 13006–10545/95 standards, on the basis of WA, ceramic tiles can be categorized into low-WA (<3%), medium-WA (3–10%), and high-WA (>10%). According to Souza et al. (2002), the specified values for WA of Brazilian clay-based products are WA < 25% and WA < 20% for dense bricks and roofing tiles, respectively. Yongue-Fouateu et al. (2016) recommended the WA ranging from 8.03 to 24.27% for quality and process control parameters in the development and manufacturing stages to produce structural ceramics. However, the low WA values (≤ 10.7%) recorded from the fired ISQW samples suggest that the materials exhibited low porosity and that the finished products would show no cracks, thereby rendering them suitable for use in the ceramics industry. The WA of the materials studied with values ≤ 10.7% at 1000°C suggested that they are suitable for use in massive-brick (WA ≤ 25%), ceramic-block (WA ≤ 25%), and roofing-tile (WA ≤ 20%) production.

The values obtained for bulk density (BD) as the firing temperature increased are presented in Table 4. The BD at 800°C ranged from 1.89 to 2.13 $g/cm^3$ while at the increased firing temperature of ~1000°C, the BD ranged from 2.0 to 2.23 $g/cm^3$. In the ceramics industry, strength variation with increasing temperature in the firing process is very important (Semiz & Çelik, 2020). From the results, strength variations that were observed in bulk-density values in all five ISQW samples tested were not significant as the temperature increased. The observed strength-variation gain obtained at 1000°C confirmed that mineralogical transformations may well have occurred (Monterio & Vieira, 2004; Tsozue et al., 2017). The level of densification exhibited by the indurated shale could be attributed to the proportions of the fluxing oxides ($Na_2O$ and $K_2O$; 4.98–7.41%) which are generally > 4.0% for each sample and this, according to Kamseu et al. (2007), often favors the formation of a vitreous phase especially at ~1100°C. The non-clay minerals such as quartz and feldspar may have further enhanced the densification of the fired ISQW materials.

The weight loss (WL) is regarded as an important feature that reveals the amount of organic matter present in the starting materials which further reflects the degree of vacuum and the percentage of water absorption. At 800°C, the WL ranged from 4.9 to 5.2% while at ~1000°C, the WL ranged from 6.3 to 8.5%. The variations observed in the WL values of all the tested ISQW samples with increased firing temperature could be attributed to the elimination of organic matter by combustion, loss of structural water, decomposition of some minerals such as sulfate and carbonate during firing (Bauluz et al., 2004; Monterio & Vieira, 2004; Tsozue et al., 2017). Tsozue et al. (2017) and Kagonbe et al. (2021) suggested that WL of < 5.0% in the weight of fired products is acceptable generally for raw materials because that serves as an added advantage in making it a cost effective material in ceramics industries but in the case of heat-treated ISQW samples, the average WL obtained was 7.0%; a value above the acceptable limit, and this suggests that the raw materials will require beneficiation.

The flexural strength (FS) of the ISQW materials ranged from 2.40 to 2.56 MPa at 800°C, while at a firing temperature of 1000°C, the FS values increased to 3.21–3.99 MPa, an indication that the technological property showed great dependence on the firing temperature. The percentages of quartz and illite present in the ISQW may have influenced the geotechnical behavior (increased FS and shrinkage) of the samples after firing. The large clay contents in the ISQW may have favored densification which resulted in more mullite formation upon firing. Densifications brought about by the large quartz contents in all of the extruded ISQW samples were assumed to be responsible for the increased flexural strength. According to Teixera et al. (2001), minimum values of flexural strength indicated for ceramics pieces at 1000°C are 2.0 MPa for massive bricks, 5.5 MPa for ceramic blocks, and 6.5 MPa for roofing tiles. The FS values (3.21–3.99 MPa) obtained from the present study at 1000°C are significantly smaller than those FS values reported by Dondi et al. (2002) for Italian brick clays as well as by other authors such as Teixera et al. (2001) and Kagonbe et al.



https://doi.org/10.1007/s42860-023-00240-w Published online by Cambridge University Press

(2021) for roofing tiles except for production of massive bricks.

### Suitability of ISQW as Raw Materials in the Production of Roofing Tiles

The present study addressed the possibility of using ISQW from Abakaliki, southeastern Nigeria, as an alternative raw material for manufacturing roofing tiles. The analytical results are consistent with a mineralogical composition dominated by quartz, illite, and chlorite with lesser amounts of feldspar and carbonate. Chemically, the major oxides present are $SiO_2$, $Al_2O_3$, $K_2O$, and CaO, with small amounts of MgO, MnO, $Fe_2O_3$, and $TiO_2$. The $SiO_2$ contents (generally $\geq$ 57.1%) in each of the tested ISQW samples are significant and, according to Zeballos et al. (2016), this is desirable for roofing-tile ceramics materials. The concentrations of MgO (0.48–0.50%) and $K_2O$ (4.98–7.41%) were due to the presence of chlorite and illite, respectively. The $Fe_2O_3$ (1.94–3.39%) and MgO (0.48–0.50%) contents were considered to be small and unlikely to impact the color of the final ceramics products. The presence of $Fe_2O_3$ and MgO is very important when the materials are being considered for use in the production of whitish tiles. The LOI (generally $\geq$ 6.43%) is significant and can be explained by the presence of clay minerals, hydroxides, and organic matter. Specifications relating to the major-oxides data are considered to be very important for ceramics applications (Diko-Makia & Ligege, 2020; Kagonbe et al., 2021). The amounts of fluxing oxides (CaO + MgO + $Fe_2O_3$ + $Na_2O$ + $K_2O$; 12.3–16.4%) are considered to be large, indicating that sufficient sintering during firing guarantees the formation of vitreous phases. Based on the chemical properties, the concentrations of $SiO_2$, $Al_2O_3$, and $Fe_2O_3$ are within the allowable international limits for ceramics formulations. The predominance of clayey-silt type materials in the ISQW samples studied means that they serve as good alternative raw materials in ceramics bodies (Semiz, 2017; Diko et al., 2011; Dondi et al., 1992). In cases where the silt contents are large, i.e. greater than the required proportions, pre-treatment such as crushing and sieving can be adopted before using the raw materials in roofing tiles (Semiz and Çelik, 2020; El Ouahabi et al., 2014). The LL (44–50%) obtained in the present study are in agreement with the range defined by Baccour et al. (2009) (30–60%) for the composition of raw materials used for ceramics production. The LL and PI values for the ISQW samples plotted on the Holtz and Kovacs (1981) diagram revealed that all the tested ISQW samples plotted within the medium- to high-plasticity region. The slight differences noted in the plasticity of the tested ISQW samples are controlled mainly by the particle size distribution data. From the Winkler and McNally diagrams, the ISQW samples studied showed heterogeneous behaviors as they plotted within vertical corrugated bricks and perforated products and bricks and tiles production, respectively.

A technological evaluation indicates the practical and technical uses of the final clay products when their properties are compared with the requirements of regulatory bodies such as the American Society for Testing Materials. Firing (heat treatment), which represents a crucial stage in the manufacture of ceramic roofing tiles, created good mechanical strength for the ISQW materials. A strong, positive correlation ($r = 0.856$, $p < 0.001$) is shown in Table 5 between sand fraction and flexural strength and between sand fraction and bulk density ($r = 0.655$, $p < 0.001$). Good positive correlation also exists ($r = 0.996$, $p < 0.001$) between LL and WA. The PI correlated well with LS ($r = 0.95$, $p < 0.001$), WA ($r = 0.856$, $p < 0.001$), and FS ($r = 0.894$, $p < 0.001$). Negative relationships exist between the clay fraction and BD ($r = –0.606$, $p < 0.001$), silt fraction and PL ($r = –0.892$, $p < 0.001$), PI and BD ($r = –0.860$, $p < 0.001$), and LL and WL ($r = –0.529$, $p < 0.001$). Very poor correlations exist between the following parameter pairs: PI and WL ($r = 0.455$, $p < 0.001$) and sand fraction and FS ($r = 0.114$, $p < 0.001$). Therefore, the physical properties of the ISQW influenced greatly the technological properties. As the firing temperature increased, the WA and WL tended to decrease while the linear shrinkage, bulk density, and flexural strength increased gradually, though increases were not significant as the firing temperature increased to 1000°C. The quartz content and illite present in the studied materials (Table 1) may have influenced the behaviors of some of the technological properties (increased FS and linear shrinkage) after firing. Illites, according to Ferrari and Gualtieri (2006), are used widely as fluxing materials in traditional ceramics for the production of cooking pots, tiles, bricks, and stoneware tiles. At the firing temperature of 1000°C, an increase in the bulk density and firing linear shrinkage were observed which agrees partially with decreased WA. After firing to ~1000°C, raw materials with FS $\geq$ 5.7 MPa (Souza et al., 2002;



https://doi.org/10.1007/s42860-023-00240-w Published online by Cambridge University Press

**Table 5** Correlations of physical properties of Albian indurated shale-quarry waste and the technological properties of fired specimens

| | Clay | Silt | Sand | LL | PL | PI | LS÷ | WA÷ | BD÷ | WL÷ | FS÷ |
|---|---|---|---|---|---|---|---|---|---|---|---|
| Clay | 1 | | | | | | | | | | |
| Silt | 0.243 | 1 | | | | | | | | | |
| | 0.694 | | | | | | | | | | |
| Sand | –0.868 | –0.677 | 1 | | | | | | | | |
| | 0.056 | 0.209 | | | | | | | | | |
| LL | 0.354 | –0.514 | –0.088 | 1 | | | | | | | |
| | 0.559 | 0.375 | 0.888 | | | | | | | | |
| PL | –0.405 | –892* | 0.790 | 0.184 | 1 | | | | | | |
| | 0.498 | 0.042 | 0.112 | 0.767 | | | | | | | |
| PI | 0.546 | 0.676 | –0.819 | 0.223 | –.917* | 1 | | | | | |
| | 0.341 | 0.211 | 0.090 | 0.718 | 0.028 | | | | | | |
| LS÷ | 0.415 | 0.729 | –0.740 | 0.000 | –.958* | .950* | 1 | | | | |
| | 0.487 | 0.162 | 0.153 | 1.000 | 0.010 | 0.013 | | | | | |
| WA÷ | 0.466 | 0.846 | –0.809 | 0.003 | –0.871 | 0.865 | 0.763 | 1 | | | |
| | 0.429 | 0.071 | 0.098 | 0.996 | 0.054 | 0.058 | 0.133 | | | | |
| BD÷ | –0.606 | –0.210 | 0.655 | –0.673 | 0.591 | –0.860 | –0.736 | –0.590 | 1 | | |
| | 0.279 | 0.735 | 0.231 | 0.213 | 0.294 | 0.062 | 0.157 | 0.295 | | | |
| WL÷ | –0.392 | 0.743 | –0.110 | –0.529 | –0.677 | 0.456 | 0.598 | 0.524 | –0.049 | 1 | |
| | 0.514 | 0.150 | 0.860 | 0.359 | 0.209 | 0.440 | 0.286 | 0.365 | 0.937 | | |
| FS÷ | –0.451 | 0.428 | 0.114 | –0.236 | –0.180 | 0.083 | 0.001 | 0.461 | 0.173 | 0.592 | 1 |
| | 0.446 | 0.472 | 0.856 | 0.703 | 0.772 | 0.894 | 0.999 | 0.435 | 0.781 | 0.293 | |

*Correlation is significant at the 0.05 level

÷Data for technological properties obtained at the high firing temperature of 1000°C

Monterio & Vieira, 2004; Onana et al., 2019) and WA < 20% (Onana et al., 2019) are considered to be valuable raw materials for roofing-tile manufacture (Table 5). The fired temperature of 1000°C served as a suitable condition for the beginning of liquid-phase sintering, increased material densification, and mechanical strength development of the raw materials for the production of roofing tiles. For the ISQW to serve well in a wide range of ceramics, convenient amendment for improved flexural strength and further reduction of the shrinkage are highly recommended. Evaluation of the technological properties suggests that ISQW materials can serve as raw materials for roofing tile manufacturing only when beneficiated in order to achieve excellent properties and to reduce the sintering temperature. With better knowledge of the physicochemical properties and technological behaviors exhibited by fired ISQW, the ceramics industries now have useful information about the raw materials at the time of formulating the ceramics pastes, thereby obtaining higher-quality products, a greater diversity of products, and a possible saving in terms of time and money in the development of the ceramics process. This research is expected to serve as a starting point and encouragement for future research and will further boost Nigeria's economy in terms of its gross domestic product and foreign-exchange earnings.

## Conclusions

Evaluation of the mineralogical, physiochemical, and ceramics properties of indurated shale-quarry wastes to determine their suitability for possible use as alternative raw materials in the ceramics (roofing tile) industry enabled the following conclusions to be drawn:

(1) The mineralogical composition of the indurated shale revealed the predominance of illite, smectite, kaolinite, and chlorite with large quantities of quartz as well as considerable percentages of



https://doi.org/10.1007/s42860-023-00240-w Published online by Cambridge University Press

carbonate and feldspar, all of which have great influence on developing ceramics materials. The chemical analyses allowed for rapid classification of the ISQW samples studied for their optimal applications. The relative abundances of $SiO_2$ were explained by the large amount of quartz while $Al_2O_3$ was correlated with clay minerals and feldspar. The proportions of $Fe_2O_3$ and MgO present in the raw materials may affect the color of the final ceramics product. Based on chemical specifications, the concentrations of $SiO_2$, $Al_2O_3$, and $Fe_2O_3$ are within the allowable international parameters for ceramics formulations.

(2) The ISQW samples classified predominantly as clayey-silt texture qualifies them for ceramics applications. Pre-treatment such as crushing and sieving can be used when the raw materials contain large proportions of silt, greater than the required proportions, before using the raw materials in structural ceramics such as roofing tiles. The LL and PI values for the ISQW samples as plotted on the Holtz and Kovacs diagram revealed that all the ISQW samples plotted in the medium-plasticity region, suggesting moderate potential for swelling. From the Winkler and McNally diagrams, the ISQW samples showed heterogeneous behaviors as they plotted within 'vertical corrugated bricks and perforated products' and 'brick and tile production,' respectively.

(3) Heat treatment of the ISQW samples, which represented a crucial stage in the manufacture of ceramics roofing tiles, created good mechanical strength for the studied raw materials. The quartz content and illite present in the ISQW influenced the mechanical characteristics (increases FS and linear shrinkage) of the tested samples after firing. The relatively large linear shrinkage agreed with the amount of smectite which can limit its applications to produce tiles. The flexural strength increased with increased firing temperature due to the formation of a dense phase. In the present study, the high firing temperature (1000°C) tended to serve as the most suitable condition for the beginning of liquid-phase sintering, increased material densification, as well as mechanical-strength development of the raw materials. Based on the technological specifications, the ISQW materials revealed acceptable weight loss, reduced shrinkage, and water absorption with unsatisfactory performances for bulk density and flexural strength ($\leq$3.99 MPa) at the elevated temperature of 1000°C in ceramics applications.

(4) The comprehensive evaluations suggest that ISQW materials can serve as raw materials for roofing-tile manufacture when beneficiated to achieve excellent properties and reduce sintering temperature. This will help to conserve existing resources, thereby enabling sustainable production in the region and reduce the production costs, especially with regard to energy consumption. With better knowledge of the technological properties of the indurated shale-quarry wastes, their use as alternative raw materials for incorporation in industrial production of roofing tiles will boost the nation's economy in terms of its gross domestic product and foreign-exchange earnings.

**Acknowledgements** The present study was supported financially in part by TETFUND. The authors acknowledge the efforts of the staff of Kaduna for their assistance during the laboratory analyses. They also acknowledge the contributions by the reviewers and the editorial team which have improved the manuscript.

**Authors' Contributions** The authors worked jointly in performing the experiments, preparing the introductory part of the manuscript, doing the main research, and arranging the manuscript to fit this journal.

**Funding** This study received partial financial support from TETFUND.

**Data Availability** We have no supplementary data or materials other than that linked above.

**Declarations**

**Ethics Approval and Consent to Participate** Approval granted.

**Conflict of Interest** There was no conflict of interest among the authors.

## References

Agumanu, A. E. (1989). The Abakaliki and Ebonyi formations: Subdivisions of the Albian Asu River Group in the southern Benue Trough, Nigeria. *Journal African Earth Sciences, 9*, 195–207.

Akande, S. O., & Muche, A. (1989). Mineralogical, textural and paragenetic studies of the lead-zinc-copper mineralization



https://doi.org/10.1007/s42860-023-00240-w Published online by Cambridge University Press

in the Lower Benue Trough (Nigeria) and their genetic implications. *Journal African Earth Sciences, 9*, 445–456.

Akintola, G. O., Amponsah-Dacosta, F., & Mhlongo, S. E. (2020). Geotechnical evaluation of clayey materials for quality burnt bricks. *Heliyon, 6*, 1–10.

Akpokodje, E. G., Ololunfemi, B. N., & Etu-Efeotor, J. O. (1991). The composition and physical properties of some ceramics and pottery clays of southeastern Nigeria. *Journal of Mining and Geology, 27*, 1–7.

ASTM C1167- 11 (2017). Standard Specification for Clay Roof Tiles.

ASTM C326 (2009). Standard test method for drying and firing shrinkages of ceramic white ware clays. ASTM International, West Conshohocken, Pennsylvania, USA.

ASTM C373 (2014). Standard test method for water absorption, bulk density, apparent porosity, and apparent specific gravity of fired whiteware products, ceramic tiles, and glass tiles. ASTM International, West Conshohocken, Pennsylvania, USA.

ASTM D422 (1972). Standard Test Method for Particle-Size Analysis of Soils.

ASTM D4318 (2010). Standard test methods for liquid limit, plastic limit, and plasticity index of soils. ASTM International, West Conshohocken, Pennsylvania, USA.

Baccour, H., Medhioub, M., Jamoussi, F., & Mhiri, T. (2009). Influence of firing temperature on the ceramic properties of Triassic clays from Tunisia. *Journal of Materials Processing Technology, 209*, 2812–2817.

Bain, J. A. (1971). A plasticity chart as an aid to the identification and assessment of industrial clays. *Clay Minerals, 9*(1), 1–17.

Baioumy, H. M., & Ismael, I. S. (2014). Composition, origin and industrial suitability of the Aswan ball clays, Egypt. *Applied Clay Science, 102*, 202–212.

Baraldi, L. (2018). World production and consumption of ceramic tiles, 2017. *Ceramic World Review*, pp, 58–72, accessed at https://www.ceramicworldweb.com/en/economics-and-markets/world-production-and-consumption-ceramic-tiles-2017 on 14th March 2023.

Bauluz, B., Mayayo, M. J., Yuste, A., Fernandez-Nieto, C., & Gonzalez Lopez, J. M. (2004). TEM study of mineral transformations in fired carbonated clays: relevance to brick making. *Clay Minerals, 39*, 333–344.

Benkhelil, J. (1989). The origin and evolution of the Cretaceous Benue Trough, Nigeria. *Journal of African Earth Science, 8*, 251–282.

Boski, T., Pessoa, J., Pedro, P., Thorez, J., Dias, J. M. A., & Hall, I. R. (1998). Factors governing abundance of hydrolysable amino acids in the sediments from the N.W. European Continental Margin (47–50°N). *Progress in Oceanography, 42*, 145–164.

Brindley, G. W. (1980). Quantitative x-ray mineral analysis of clays. In G. W. Brindley & G. Brown (Eds.), *Crystal structures of clay minerals and their x-ray identification,* Monograph 5 (pp. 411–438). London: Mineralogical Society.

Brindley, G.W. & Brown, G. (1980). *Crystal Structures of Clay Minerals and Their X-ray Identification*. Mineralogical Society Monograph 5, (3rd ed.). Mineralogical Society, London.

Bun Kim, N., Hasmaliza, M., Shamsul, K. S., Kiyoshi, O., & Zainal, A. A. (2011). Some ceramic properties of clays from central Cambodia. *Applied Clay Science, 53*, 33–41.

Burke, K., Dessauvagie, T. F. J., & Whiteman, A. J. (1971). Opening of the Gulf of Guinea and geological history of the Benue Depression and Niger Delta. *Nature and Physical Sciences, 233*(38), 51–55.

Casagrande, A. (1947). Classification and identification of soils. *American Society of Civil Engineers Proceedings, 73*(6), 783–810.

Celik, H. (2010). Technological characterization and industrial application of two Turkish clays for the ceramic industry. *Applied Clay Science, 50*, 245–254.

Chen, Y., Zhang, Y., Chen, T., Zhao, Y., & Bao, S. (2011). Preparation of eco-friendly construction bricks from hematite tailings. *Construction and Building Materials, 25*, 2107–2111.

Çolak, M., & Özkan, İ. (2011). Sintering properties of the Bornova shale (Turkey) and its application in the production of red fired ceramics. *Industrial Ceramics, 31*(3), 209–215.

Cook, H.E., Johnson, P.D., Matti, J.C., & Zemmels, I. (1975). Methods of sample preparation and X-ray diffraction data analysis. X-ray mineralogy laboratory. Pp. 999 – 1007 in: *Initial Report DSDP* (D.E. Hayes, L.A Frakes et al., editors), *28.*

Cratchley, C., & Jones, G. P. (1965). An interpretation of the geology and gravity anomalies of the Benue Valley, Nigeria. Overseas geological Survey Geophysics, P. 1. *Geological Magazine, 118*, 59–67.

Daoudi, L., Elboudour, E. H., Saadi, L., Albizane, A., Bennazha, J., Waqif, M., El Ouahabi, M., & Fagel, N. (2014). Characteristics and ceramic properties of clayey materials from Amezmiz region (Western High Atlas, Morocco). *Applied Clay Science, 102*, 139–147.

Diko-Makia, L., & Ligege, R. (2020). Composition and technological properties of clays for structural ceramics in Limpopo (South Africa). *Minerals, 10*(8), 700.

Diko, M. L., Ekosse, G. I., Ayonghe, S., & Ntasin, E. B. (2011). Physical characterization of clayey materials from tertiary volcanic cones in Limbe (Cameroon) for ceramic applications. *Applied Clay Science, 51*, 380–384.

Dondi, M., Ercolani, G., Guarani, G., & Raimondo, M. (2002). Orimulsion fly ash in clay bricks. Part 1: Composition and thermal behavior of ash. *Journal of the European Ceramics Society, 22*, 1729–1735.

Dondi, M., Raimondo, M., & Zanelli, C. (2014). Clays and bodies for ceramic tiles: Reappraisal and technological classification. *Applied Clay Science, 96*, 91–109.

Ekosse, G. E. (2010). Kaolin deposits and occurrences in Africa: Geology, mineralogy and utilization. *Applied Clay Science, 50*, 212–236.

El Ouahabi, M., Daoudi, L., & Fagel, N. (2014). Mineralogical and geotechnical characterization of clays from northern Morocco for their potential use in the ceramic industry. *Clay Minerals, 49*, 35–51.

Fagel, N., Boski, T., Likhoshway, L., & Oberhaensli, H. (2003). Late Quaternary clay mineral record in Central Lake Bikal (Academician Ridge, Siberia). *Paleogeography, Paleoclimatology, Paleoecology, 193*, 159–179.

Ferrari, S., & Gualtieri, A. F. (2006). The use of illitic clays in the production of stoneware tile ceramics. *Applied Clay Science, 32*, 73–81.

Fiori, C., Fabbri, B., Donati, G., & Venturi, I. (1989). Mineralogical composition of the clay bodies used in the Italian tile industry. *Applied Clay Science, 4*, 461–473.



https://doi.org/10.1007/s42860-023-00240-w Published online by Cambridge University Press

Galan, H. E. (2003). *Mineralogia Aplicada* (1st ed.). Sintesis. 399 pp.
Garcia-Valles, M., Alfonso, P., Martinez, S., & Roca, N. (2020). Mineralogical and thermal characterization of Kaolinitic clays from Terra Alta (Catalonia, Spain). *Minerals, 10*, 142.
Gonzales, G. F., Romero, A. V., Garcia, R. G., & Gonzales, R. M. (1990). Firing transformation of mixtures of clays containing illite, kaolinite and calcium carbonate used by ornamental tile industries. *Applied Clay Science, 5*(4), 361–375.
Heiri, O., Lotter, A. F., & Lemcke, G. (2001). Loss on ignition as a method for estimating organic and carbonate content in sediments: Reproducibility and comparability of results. *Journal of Paleolimnology, 25*, 101–110.
Holtz, R. D., & Kovacs, W. D. (1981). *An Introduction to Geotechnical Engineering*. Prentice-Hall Inc.
Huber, J. M. (1985). *Kaolin Clays*. Huber Corporation (Clay Division). 64 pp.
Kagonbe, B. P., Tsozue, D., Nzeukou, A. N., & Ngos, S. (2021). Mineralogical, physico-chemical and ceramic properties of clay materials from Sekande and Gashiga (North, Cameroon) and their suitability in earthenware production. *Heliyon, 7*, 1–10.
Kamseu, E., Leonelli, C., Boccaccini, D. N., Veronesi, P., Miselli, P., & Pellacani, G. (2007). Characterisation of porcelain compositions using two china clays from Cameroon. *Ceramics International, 33*, 851–857.
Kazmi, S. M. S., Abbas, S., Saleem, M. A., Munir, M. J., & Khitab, A. (2016). Manufacturing of sustainable clay bricks: Utilization of waste sugarcane bagasse and rice husk ashes. *Construction and Building Materials, 120*, 29–41.
Keller, W. D. (1968). Flint clay and flint-clay facies. *Clays and Clay Minerals, 16*, 113–128.
Kühnel, R. A. (1990). The modern clays of clays. *Applied Clay Science, 5*, 135–143.
Lambercy, E. (1993). Les matieres premieres ceramiques et leur transformation par le feu. Granit, Vol. 1 des Dossiers Argiles, France, p. 509.
Lingling, X., Wei, G., Tao, W., & Nanru, Y. (2005). Study on fired bricks with replacing clay by fly ash in high volume ratio. *Construction Building Materials, 9*, 243–247.
Lori, E.A. (2008). Feldspars and Nepheline Syenite. USGS Minerals, Yearbook.
Mahmoudi, S. Z. (2008). The use of Tunisian Barremian clay in the traditional ceramic industry: Optimization of ceramic properties. *Applied Clay Science, 42*, 125–129.
Manukaji, J. U. (2013). Chemical and mechanical characterization of clay samples from Kaduna State Nigeria. *IJEI, 2–7*, 20–26.
Marsigli, M., & Dondi, M. (1997). Plasticita delle Argille Italiane per Laterizi e Previsione Del Loro Comportamento in Foggiatura. *L'industria Laterizi, 46*, 214–222.
McNally, G. H. (1998). *Soil and Rock Construction Materials* (pp. 291–310). CRC Press.
Moharem, A. F., & Saleh, A. E. M. (2007). Properties and suitability of Wadi Zarieb Feldspars for ceramic industries in Egypt. *Journal of Applied Science, 7*(19), 2794–2799.
Monterio, S. N., & Vieira, C. M. F. (2004). Influence of firing temperature on the ceramic properties of clays from Campos dos Goytacazes, Brazil. *Applied Clay Science, 27*, 229–234.
Moore, D. M., & Reynolds, R. C. (1989). *X-ray Diffraction and the identification and analysis of clay minerals*. Oxford University Press. 332 pp.
Murray, H. H. (2000). Traditional and new applications for kaolin, smectite, palygorskite: A general overview. *Applied Clay Science, 17*, 207–221.
Murray, H.H. (2007). *Applied Clay Mineralogy: Occurrences, Processing and Application of Kaolins, Bentonites, Palygorskite–Sepiolite and Common Clays.* Developments in Clay Science; Elsevier, Amsterdam*, 2,* 179 pp.
Ngun, B. K., Mohamad, H., Sulaiman, S. K., Okada, K., & Ahmad, Z. (2011). Some ceramic properties of clays from central Cambodia. *Applied Clay Science, 53*, 33–41.
Nwajide, C. S. (2013). *Geology of Nigeria's Sedimentary Basins* (p. 565). CSS Bookshops Ltd.
Nwajide, C.S. (1990). Cretaceous sedimentation and paleogeography of the central Benue Trough. In: Ofoegbu C.O. (Ed). The Benue Trough structure and evolution. *Earth Evolution series, viewing*, *Germany*. Pp. 77–91.
Nweke, O. M., & Okogbue, C. O. (2017). The potential of cement stabilized shale quarry dust for possible use as road foundation material. *International Journal of Geo-Engineering, 8*(29), 1–14.
Nweke, O. M., & Okogbue, C. O. (2021). Mechanical and Performance-related properties of bitumen-beneficiated indurated shale aggregates for use in road construction in southeastern Nigeria. *Bulletin of Engineering Geology and Environment, 80*(12), 9141–9156.
Obiora, S. C., & Charan, S. N. (2011). Geochemistry of Regionally metamorphosed sedimentary rocks from the Lower Benue Rift: Implications for provenance and tectonic setting of the Benue Rift sedimentary suite. *South African Journal of Geology, 1*, 25–40.
Odoma, A. N., Obaje, N. G., Omada, J. I., Idakwo, S. O., & Erbacher, J. (2015). Mineralogical, chemical composition and distribution of rare earth elements in clay-rich sediments from southeastern Nigeria. *Journal of African Earth Sciences, 102*, 50–60.
Okogbue, C. O., & Nweke, O. M. (2018). The $^{226}$Ra, $^{232}$Th and $^{40}$K contents in the Abakaliki baked shale construction materials and their potential radiological risk to public health, southeastern Nigeria. *Journal of Environmental Geology, 2*(1), 13–19.
Olade, A. M. (1979). Evolution of Nigeria's Benue Trough (Aulacogen) a tectonic model. *Geological Magazine, 112*, 575–593.
Onana, V. L., Ntouala, R. F. D., Mbey, J. A., Ngo'oZe, A., Kabeyene, V. K., & Ekodeck, G. E. (2019). Mineralogy and preliminary assessment of the potential uses of alluvial clays from Batouri (Eastern-Cameroon). *Cerâmica, 65*, 407–415.
Oyebanjo, O., Ekosse, G., & Odiyo, J. (2020). Physico-chemical, mineralogical, and chemical characterisation of cretaceous–Paleogene/Neogene Kaolins within Eastern Dahomey and Niger Delta Basins from Nigeria: Possible industrial applications. *Minerals, 10*, 670.
Özkan, İ. (2014). Ceramic properties of a Turkish clay in the Aydin region. *Journal of Ceramic Processing Research, 15*(1), 44–47.

Parker, E. R. (1967). *Materials Data Book for Engineers and Scientists*. Publ. McGraw Hill Book Co. 283 pp.
Pavlova, I.A., Kutasheva, S.S., & Farafontova, E.P. (2019). Production technology of ceramic roof tiles based on raw materials of Ural region, IOP Conf. Series: *Materials Science and Engineering,* 687, 022022.
Peters, T., & Iberg, R. (1978). Mineralogical changes during firing of calcium-rich brick clays. *American Ceramic Society Bulletin, 57*(5), 503–506.
Pontikes, Y., Espósito, L., Tucci, A., & Angelopoulos, G. N. (2007). Thermal behavior of clays for traditional ceramics with soda–lime–silica waste glass admixture. *Journal of the European Ceramics Society, 27*, 1657–1663.
Revuelta, M.B. (2021). Construction materials; Geology, Production and Applications. Springer Nature AG, Switzerland.
Reyment, R. A. (1965). *Aspects of the Geology of Nigeria* (p. 154). University Press.
Rieder, M., Cavazzini, G., Dyakonov, Y. S., Frank-Kamenetskii, V. A., Gottardi, G., Guggenheim, S., Koval, P. V., Müller, G., Neiva, A. M. R., Radoslovich, E. W., Robert, J.-L., Sassi, F. P., Takeda, H., Weiss, Z., & Wones, D. R. (1998). Nomenclature of micas. *Clays and Mineralogy, 46*, 586–595.
Ripoli, F. (1997). The use of industrial ceramic waste - Brick Powder - to improve product quality in ceramic elements manufacture: An experimental study. *Cerâmica, 43*, 281–282.
Rooney, D. (1984). *Khmer Ceramics*. Oxford University Press.
Semiz, B. (2017). Characteristics of clay-rich raw materials for ceramic applications in Denizli region (Western Anatolia). *Applied Clay Science, 137*, 83–93.
Semiz, B., & Çelik, S. B. (2020). Mineralogical and geochemical characteristics of Belevi clay deposits at Denizli, SW Turkey: Industrial raw material potential. *Arabian Journal of Geosciences, 13*, 313.
Simpson A (1954). The Nigerian coalfield. The geology of parts of Onitsha, Owerri and Benue provinces. *Bulletin Geological Survey Nigeria*, *24*(8), p 85
Serra, M. F., Conconi, M. S., Suarez, G., Agietti, E. F., & Rendtor, N. M. (2013). Firing transformations of an Argentinean calcareous commercial clay. *Cerâmica, 59*, 254–261.
Singer, F., & Sonja, S. S. (1971). *Industrial Ceramics* (p. 56). Chapman & Hall.
Skempton, A. W., & Northey, R. D. (1952). The sensitivity of clays. *Geotechnique, 3*, 30.
Skempton, A.W. (1953). The colloidal activity of clays. In: *Proceedings of the 3rd international conference on soil mechanics*, Zurich, pp. 57–61.
Souza, G. P., Sanchez, R., & De Holanda, J. N. F. (2002). *Cerâmica, 48*(306), 102.
Stock, D. (2012). *World Production and Consumption of Ceramic Tile Today, 77*, 30–37.
Strazzera, B., Dondi, M., & Marsigli, M. (1997). Composition and ceramic properties of tertiary clays from southern Sardinia (Italy). *Applied Clay Science, 12*, 247–266.
Subashi De Silva, G. H. M. J., & Malwatta, M. P. D. P. (2018). Strength, durability, thermal and run-off properties of fired clay roof tiles incorporated with ceramic sludge. *Construction and Building Materials, 179*, 390–399.
Teixera, S. R., Souza, S. A., & Moura, C. A. (2001). Mineralogical characterization of clays used in the structural ceramic industry in West of Sao Paulo State, Brazil. *Cerâmica, 47*, 204–207.
Temga, J. P., Mache, J. R., Madi, A. B., Nguetnkam, J. P., & Bitom, D. L. (2019). Ceramics applications of clay in Lake Chad Basin, Central Africa. *Applied Clay Science, 171*, 118–132.
Terrones-Saeta, J. M., Suárez-Macías, J., Iglesias-Godino, F. J., & Corpas-Iglesias, F. A. (2020). Study of the incorporation of biomass bottom ashes in ceramic materials for the manufacture of bricks and evaluation of their leachates. *Materials, 13*, 2099.
Tsozue, D., Nzeukou, N. A., Mache, J. R., Loweh, S., & Fagel, N. (2017). Mineralogical, physico-chemical and technological characterization of clays from Maroua (Far-North, Cameroon) for use in ceramic bricks production. *Journal of Building and Engineering, 11*, 17–24.
Viani, A., Cultrone, G., Sotiriadis, K., Ševˇcík, R., & Sasek, P. (2018). The use of mineralogical indicators for the assessment of firing temperature in fired-clay bodies. *Applied Clay Science, 163*, 108–118.
Winkler, H. G. F. (1954). Bedeutung der Korngrössenverteilung und des Mineralbestandes von Tonen für die Herstellung grobkeramischer Erzeugnisse. *Berichte Der Deutschen Keramischen Gesellschaft, 31*, 337–343.
Yongue-Fouateu, R., Ndimukong, F., Njoya, A., Kunyukubundo, F., & Mbih, P. K. (2016). The Ndop plain clayey materials (Bamenda area—NW Cameroon): Mineralogical, geochemical, physical characteristics and properties of their fired products. *Journal of the Asian Ceramics Society, 4*, 299–308.
Zeballos, A., Weihed, P., Blanco, M., & Machaca, V. (2016). Geological, mineralogical and chemical characterization of Devonian kaolinite-bearing sediments for further applications in the ceramic (tiles) industry in La Paz, Bolivia. *Environmental Earth Sciences, 75*, 546.





https://doi.org/10.1007/s42860-023-00240-w Published online by Cambridge University Press